Electronic Supplementary Information

Preparation of native β-cyclodextrin modified plasmonic hydrogel substrate and its use as a surface-enhanced Raman scattering scaffold for antibiotics identification

Lei Ouyang,[a,b] Lihua Zhu,*[,a] Yufeng Ruan[b], Heqing Tang*[,b]

[a] School of Chemistry and Chemical Engineering, Huazhong University of Science and Technology, Wuhan 430074, P. R. China

[b] Key Laboratory of Catalysis and Materials Science of the State Ethnic Affairs Commission and Ministry of Education, College of Resources and Environmental Science, South Central University for Nationalities, Wuhan 430074, P. R. China

Corresponding Authors: Professor Lihua Zhu, School of Chemistry and Chemical Engineering, Huazhong University of Science and Technology, Wuhan 430074, P. R. China. Tel/Fax: +86 27 87543632. E-mail: lhzhu63@hust.edu.cn. Professor Heqing Tang, College of Resources and Environmental Science, South Central University for Nationalities, Wuhan 430074, P. R. China. Tel/fax: +86-27-67843323. E-mail: tangheqing@mail.scuec.edu.cn, hqtang62@aliyun.com (H. Tang).

Optimization of reduction time and temperature for preparing CD-Ag NPs

When Ag salt was added to the alkaline solution of β-CD, the initial colorless solution was rapidly turned to brown. This was followed by in situ reducing of Ag^+ to zero-valence Ag by hydroxyl group, exhibiting bright yellow color. The gradual darkening of the solution in color showed the subsequent growth of β-CD bound Ag clusters into larger Ag NPs. The reducing process was monitored by the UV-vis absorption spectroscopy. It was found that as the reduction time was prolonged, a strong symmetric absorption peak occurred at about 416 nm and increased in intensity (Figure. S1a), being attributed to the surface plasmon resonance (SPR) peak with C_s symmetry of sphere Ag particles. The intensity of the absorption peak was increased to maximum at 60 min. When prolonging the reaction time beyond 60 min, the absorbance increased little, signing the completion of the reduction process. Therefore, the reduction time was set to 60 min in following experiments. Similarly, the effects of reduction temperature on the generation of CD-Ag sols were checked, and the synthesis of CD-Ag NPs was not markedly influenced by the reaction time ranging from 60 °C to 90°C (Figure. S1b). Therefore, the reduction temperature was set at 60 °C for synthesizing CD-Ag.

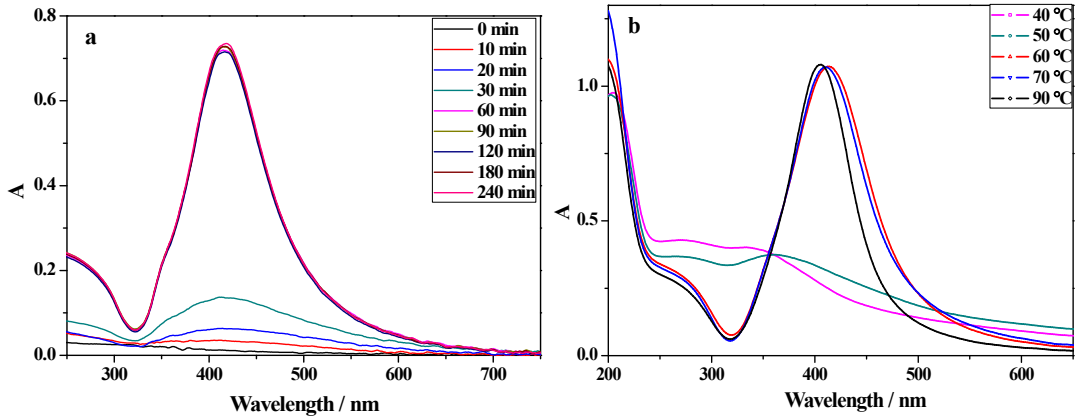

Figure S1. (a) Time dependence of UV-vis absorption spectra of CD-Ag sol during the synthesis.(b) UV-vis absorption spectra of CD-Ag sol synthesized at different reaction temperatures.

Optimization of reaction pH for preparing CD-Ag NPs

Solution pH also influenced on the formation of Ag NPs (Figure S2 and Table S1). When the pH < 9.15, no SPR peak of Ag NPs was observed, which means that the reduction of Ag^+ in this system required a solution pH higher than pH 9.15.When pH was increased to 10.28, a weak broad peak was observed at 420 nm, showing the formation of Ag NPs with somewhat broad size distribution. When pH was increased to 11.83 and more, a strong sharp peak appeared around 415 nm, demonstrating an efficient formation of Ag NPs. It should be noted that the peak was broadened at initial pH 13.01, indicating a widened size distribution of Ag NPs, possibly due to the increased aggregation at over-high pH. Indeed, the stability of the sol of Ag NPs was the best when the initial pH was controlled in the pH range of 11.8–12.2, at which the Ag NP sol could keep stable after storage for more than 6months. Therefore, the initial solution pH was selected at pH 12.0±0.2.

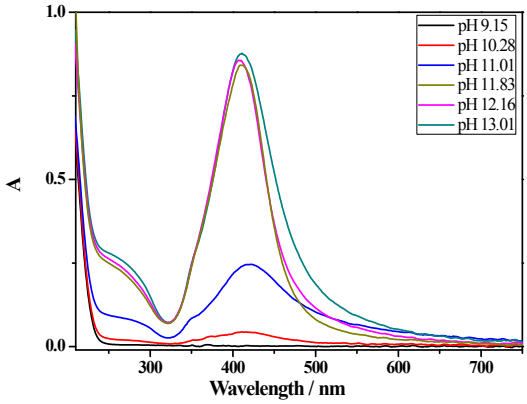

Figure S2.UV-vis absorption spectra of CD-Ag sol with different initial pH values for the synthesis.

Table S1. Solution pH changes before and after the synthesis of CD-Ag with different initial pH values

No.	Initial pH	Final pH
1	9.15	6.98
2	10.28	6.63
3	11.01	7.08
4	11.83	11.26
5	12.16	11.96
6	13.01	12.98

Optimization of the concentrations of β-CD and Ag^+ in the synthesis of β-CD-capped Ag NPs

The Ag NPs were produced by the reducing action of β-CD, and hence the molar ratio of β-CD to Ag^+ affected on the size and stability of the CD-Ag NPs. The influence of the concentration of β-CD was investigated by fixing the initial Ag^+ concentration at 1.25 mM. When the concentration of β-CD was increased from 0.25 mM to 6.25 mM (the molar ratio of β-CD to Ag^+: 0.2:1 to 5:1), the maximum absorption wavelength of the CD-Ag NP sol was blue shifted from 420 nm to 407 nm (Figure. S3a). The blue shift of the SPR peak represented a decrease of the particle sizes of CD-Ag NPs as confirmed by the particle size analysis (Figure. S3a). Similarly, the influence of Ag^+ concentration was studied on the formation of CD-Ag NPs by fixing the concentration of β-CD at 1.25mM (Figure. S3b). It was observed that the SRP peak was increased in intensity without peak wavelength shift with increasing the concentration of Ag^+ from 0.25 mM to 2.5 mM, which means that the yield of CD-Ag NPs was increased while the particles size did not markedly change. However, only black precipitates were produced when the concentration of Ag^+ was higher than 2.5 mM, due to the formation of AgOH or Ag_2O precipitates. Therefore, the initial concentrations of the reactants for the synthesis of CD-Ag NPs were set at 1.25 mM Ag^+ and 1.25 mM β-CD in next experiments.

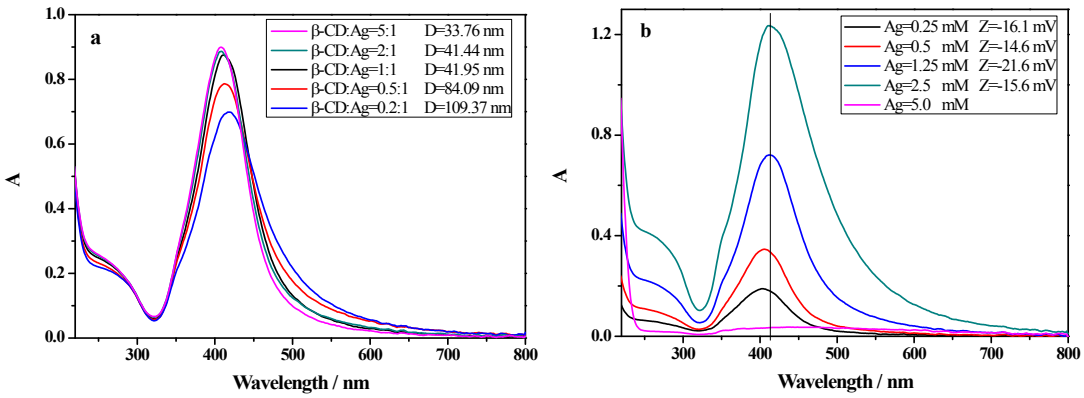

Figure S3. (a) UV-vis absorption spectra of CD-Ag sol synthesized with different β-CD concentrations. The D values were the diameter of the Ag NPs measured by laser particle analyzer. (b)UV-vis absorption spectra of CD-Ag sol synthesized different $AgNO_3$ concentrations. The Z values gave the Zeta potentials of the Ag NPs.

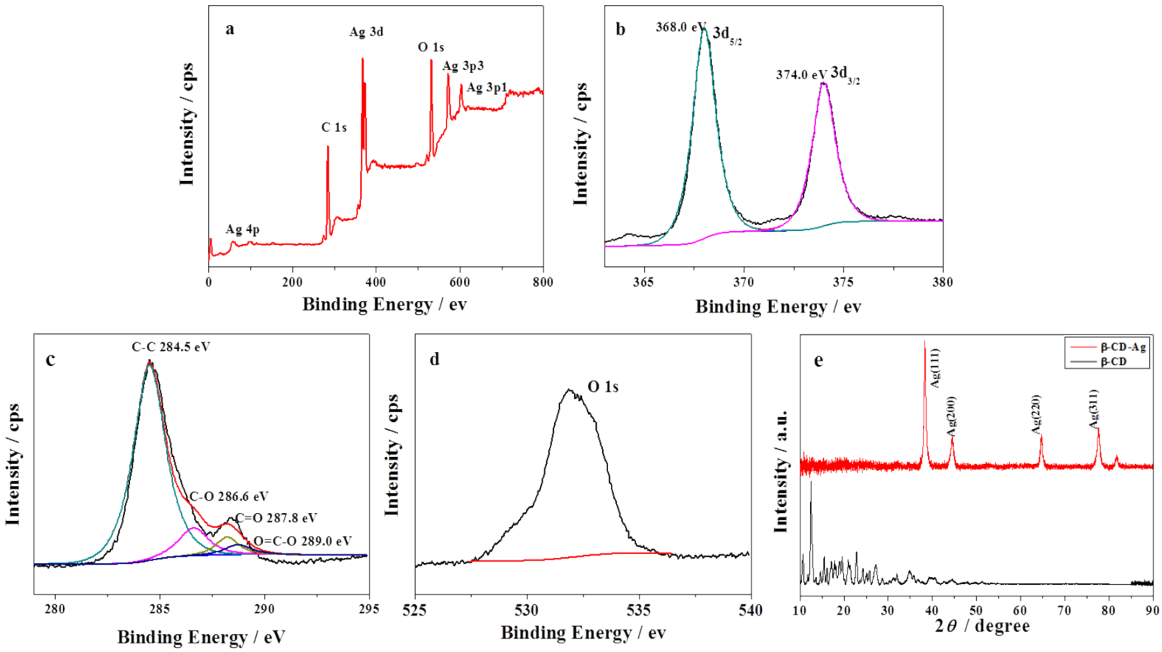

Figure S4. (a-d) XPS spectra of CD-Ag NPs:(a) wide survey XPS spectrum, (b) XPS Ag3d envelop, (c) XPS C 1s envelop, and (d) XPS O 1s envelop. (e) XRD spectra of CD-Ag NPs and β-CD powder.

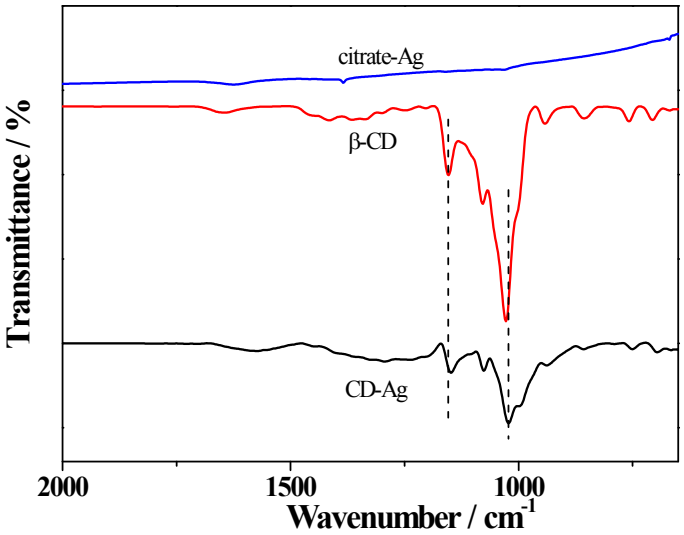

Figure S5. FTIR spectra of citrate-Ag NPs, β-CD powder and CD-Ag NPs.

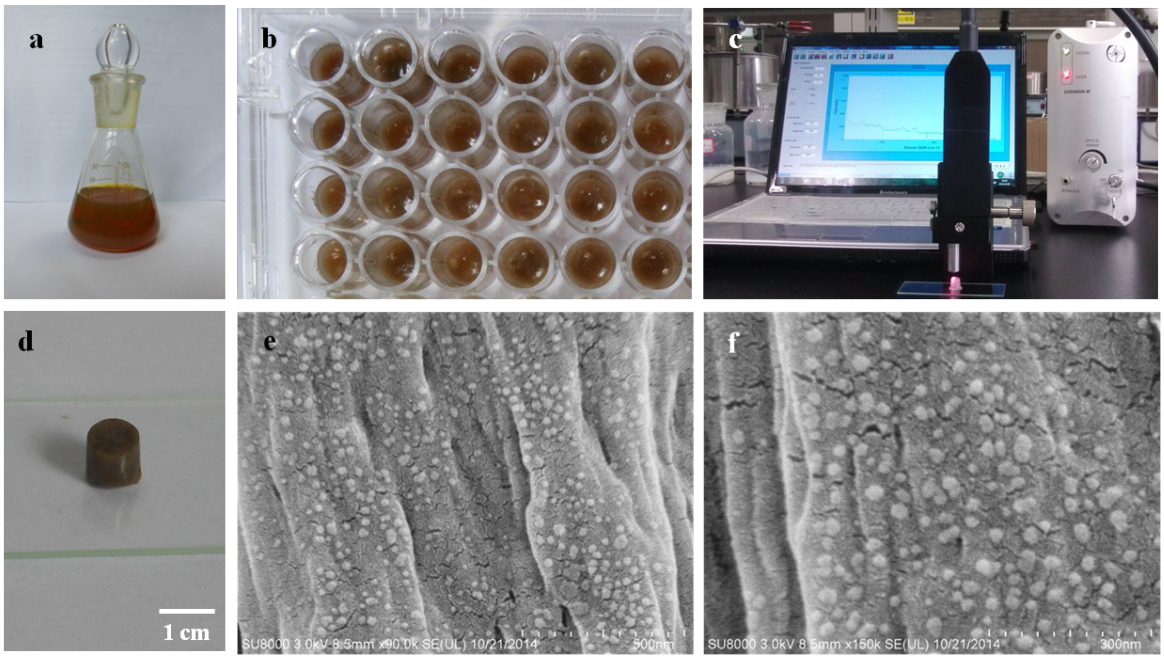

Figure S6. Optical observations for CD-Ag sol and PVA-CD-Ag hydrogel. (a) CD-Ag sol before gelation ; (b) PVA-CD-Ag hydrogel in 96-well plate; (c) SERS detection of analytes with PVA-CD-Ag hydrogel by potable Raman instrument; (d) The close-up photography for PVA-CD-Ag hydrogel; (e) and (f) SEM images of PVA-CD-Ag hydrogel, where the scale bar was 500 nm and 300 nm, respectively.

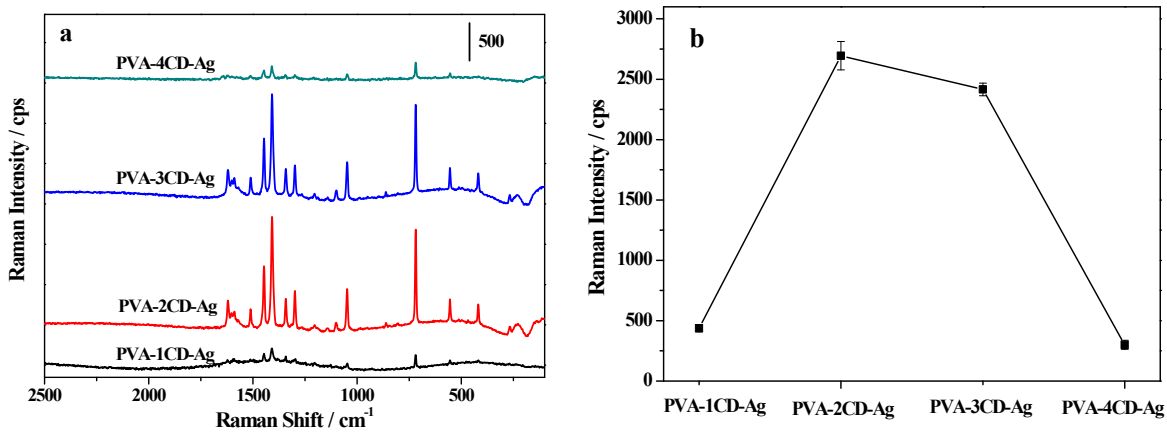

Figure S7. (a) SERS spectra and (b) the 1409 cm^{-1} peak intensity of 1,10-phenanthroline (5×10^{-5} mol L^{-1}) on PVA-1CD-Ag, PVA-2CD-Ag, PVA-3CD-Ag, and PVA-4CD-Ag.

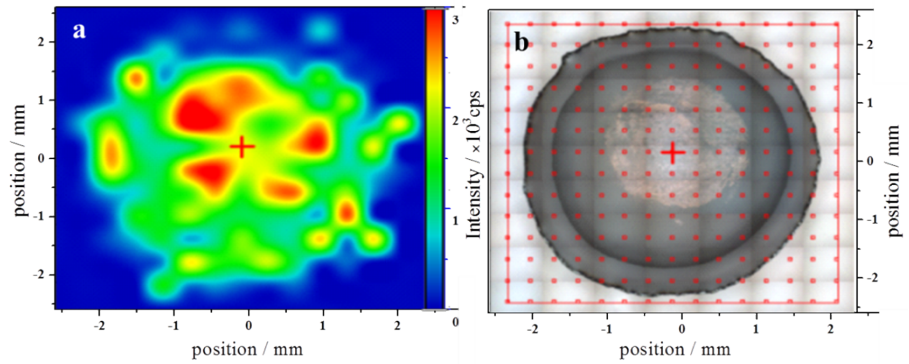

Figure S8. Map-scanning of 20 μL CD-Ag sol dripped onto a slide (pre-adsorbed with 5×10^{-5} mol L^{-1} 1,10-phenanthroline). (a) SERS intensity map at 1409 cm^{-1}. (b) White light image of the scanned area of PVA-CD-Ag.

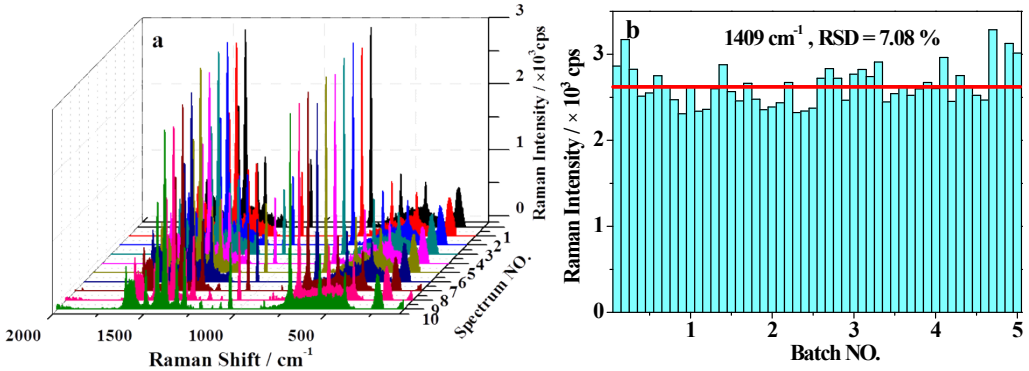

Figure S9. The reproducibility of PVA-CD-Ag substrate. (a) SERS spectra of 1,10-phenanthroline (5×10^{-5} M) on PVA-CD-Ag recorded at 10 spots randomly chosen (see the spot number). (b) SERS intensity (at the 1409 cm^{-1} peak) of 1,10-phenanthroline (5×10^{-5}mol L^{-1}) on different PVA-CD-Ag substrates. The different PVA-CD-Ag substrates were prepared in 5 batches, and the spectrum recording was conducted at 10 spots randomly chosen for each batch substrate. The blue line signed the average intensity of the 10×5 measurements, with a RSD of 7.08%.

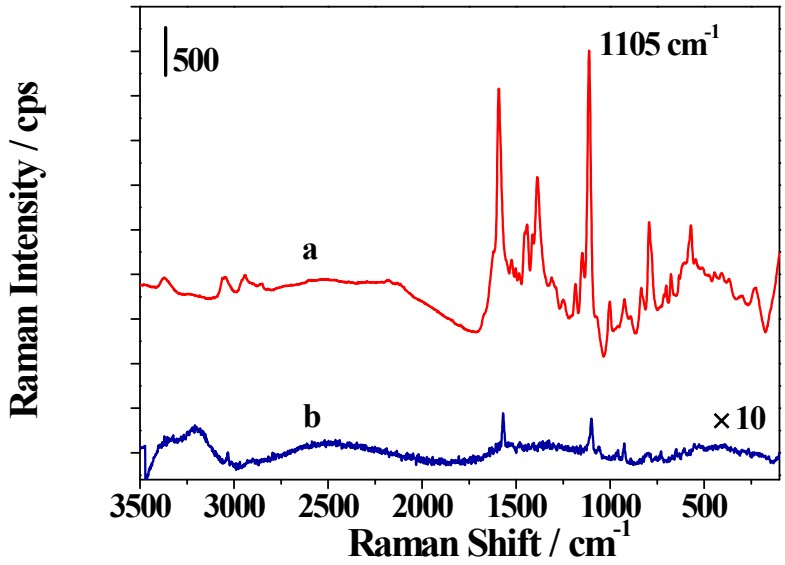

Figure S10. SERS and Raman spectra for enhancement factor calculation. (a) SERS spectrum of 3.6×10^{-5} mol L^{-1} SMM with PVA-CD-Ag as substrate, and (b) Raman spectrum of 1 mol L^{-1} SMM.

Enhancement Factor (EF) was calculated by using the standard formula, [1]

$$EF=(I_{SERS}/C_{SERS})\times(C_{NR}/I_{NR})$$

where I_{SERS} and I_{NR} are the intensity at the chosen wavenumber in obtained SERS and normal Raman spectrum, respectively. C_{SERS} and C_{NR} are the concentration of analytes used for SERS and normal Raman scattering measurements, respectively. The most intense peak (1105 cm^{-1}) was considered for EF calculation,

$$EF=(2610.04/3.6\times10^{-5})\times(1/33.02)$$

The EF was calculated to about 1.97×10^{6}.

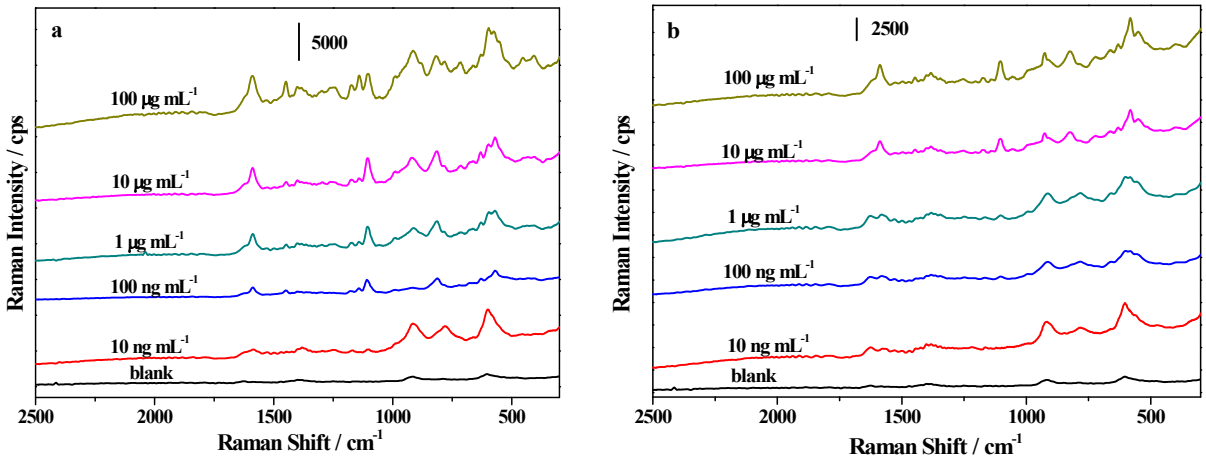

Figure S11. SERS spectra of (a) sulfadiazine (SD), and (b) sulfadimidine (SDD) in water at different concentrations.

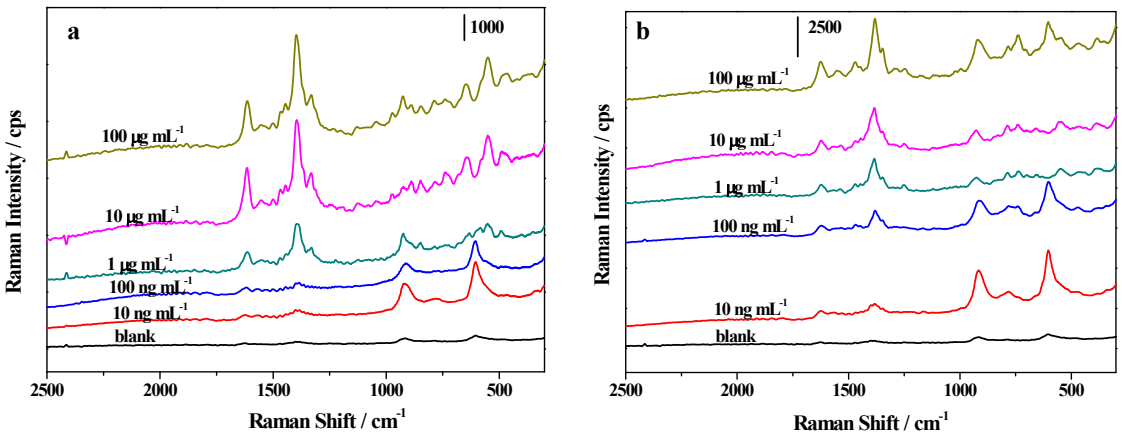

Figure S12. SERS spectra of (a) ofloxacin and (b) enrofloxacin in water at different concentrations in ultra-pure water.

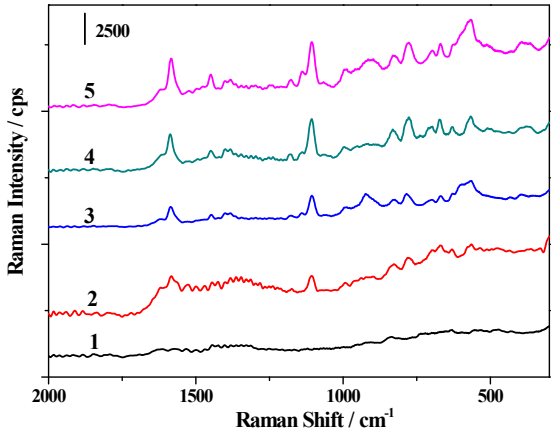

Figure S13. SERS spectrum of lake water and its spiked samples with SMM: (1) lake water; (2) lake water spiked with 1 μg mL^{-1} SMM;(3) 1μg mL^{-1} SMM solution; (4) lake water spiked with 10 μg mL^{-1} SMM; (5) 10 μg mL^{-1} SMM solution.

Table S2 Determination of sulfonamides in lake water and lab wastewater samples

Sample	Analyte	Found (μg mL^{-1}) by HPLC	Added (μg mL^{-1})	Found (μg mL^{-1}) by SERS	Recovery (%)
Lake water	SMM	0	10.0	9.2	92.7
	SD	0	10.0	11.4	114.3
	SDD	0	10.0	9.4	94.3
Lab wastewater	SMM	12.5		11.8	
	SD	10.4		8.9	
	SDD	15.6		15.0	

References

[1] I. Chakraborty, S. Bag, U. Landman, and T. Pradeep, *J. Phys. Chem. Lett.* 2013, **4**, 2769.